Journal of Cellular Biochemistry 101:1301–1315 (2007)

Subcellular Localization of Ankyrin Repeats Cofactor-1 Regulates Its Corepressor Activity

Aihua Zhang, Chia-Wei Li, Shih-Chieh Tsai, and J. Don Chen*

Department of Pharmacology, University of Medicine and
Dentistry of New Jersey-Robert Wood Johnson Medical School, Piscataway, New Jersey

Abstract The ankyrin repeats cofactor-1 (ANCO-1) was recently identified as a novel nuclear receptor corepressor that regulates receptor-mediated transcription through interactions with p160 coactivators and histone deacetylases. Interestingly, exogenously expressed ANCO-1 is localized at distinct subnuclear domains. The relevance of these subnuclear domains and the mechanisms of nucleocytoplasmic translocation of ANCO-1 have not been determined. We report here the identification of an N-terminal signaling motif that is essential for both nuclear/subnuclear localization and transcription corepressor function of ANCO-1. This N-terminal motif at residues 80–86 of ANCO-1 constitutes a classical nuclear localization signal (NLS1). Disruption of NLS1 causes complete cytoplasmic accumulation of the full-length ANCO-1, and abolishes its corepressor function on receptor-mediated transcription. A second NLS (NLS2) is found at the C-terminal residues 2384–2390; however, its disruption abolishes only nuclear localization of isolated C-terminal fragments. We also identify a leucine-rich nuclear export signal (NES) at residues 2415–2424 of ANCO-1, and show that both the NLSs and NES sequences are capable of mediating nuclear import and export of heterologous protein, respectively. In addition, attachment of the NES sequence to a transcription factor impairs its activation function. These results suggest that ANCO-1 subnuclear localization is regulated by both nuclear import and export signals, and that proper subcellular localization of ANCO-1 is essential for its corepressor function. J. Cell. Biochem. 101: 1301–1315, 2007.

Key words: NLS; NES; coactivators; corepressors; progesterone receptor; ANCO-1; p160

Nuclear receptors (NRs) are DNA-binding transcription factors that regulate hormone-dependent gene expression in many important biological processes, including development and reproduction [Nawaz et al., 1994; Mangelsdorf et al., 1995]. NR coactivators and corepressors are known to mediate the transcriptional activation and repression functions of NRs, respectively. Among the known corepressors, SMRT and N-CoR are highly related and bind primarily to unliganded NRs [Chen and Evans, 1995; Horlein et al., 1995; Ordentlich et al., 1999; Park et al., 1999]. SMRT and N-CoR mediate transcriptional repression through recruitment of histone deacetylases (HDACs) [Nagy et al., 1997; Guenther et al., 2000; Li et al., 2000]. Conversely, the p160 family of NR coactivators bind to liganded NRs to mediate transcriptional activation through recruitment of histone acetyltransferases (HAT) [Leo and Chen, 2000]. The p160 family members include SRC-1 [Oñate et al., 1995], TIF2/GRIP1 [Hong et al., 1996, 1997; Voegel et al., 1996], and RAC3/ACTR/AIB1/pCIP/TRAM-1 [Anzick et al., 1997; Chen et al., 1997; Li et al., 1997; Takeshita et al., 1997; Torchia et al., 1997]. The SMRT/N-CoR corepressors and the p160 coactivators bind to a common hydrophobic groove on the receptor through distinct LXXLL motifs [Heery et al., 1997; Shiau et al., 1998; Ghosh et al., 2002; Xu et al., 2002]. Genetic studies

This article contains supplementary material, which may be viewed at the Journal of Cellular Biochemistry website at http://www.interscience.wiley.com/jpages/0730-2312/suppmat/index.html.

Abbreviations used: ANCO-1, ankyrin repeats containing cofactor-1; RAC3, receptor-associated coactivator-3; NLS, nuclear localization signal; NES, nuclear export signal; PR, progesterone receptor.

Grant sponsor: NIH; Grant numbers: DK52888, DK52542, CA87074.

*Correspondence to: J. Don Chen, Department of Pharmacology, UMDNJ-Robert Wood Johnson Medical School, 661 Hoes Lane, Piscataway, NJ 08854-5635.
E-mail: chenjd@umdnj.edu

Received 29 November 2006; Accepted 1 December 2006
DOI 10.1002/jcb.21251

further confirm p160 coactivators as being critically involved in regulating hormonal responses in mice [Xu et al., 1998, 2000; Wang et al., 2000]. Among members of the p160 coactivators, RAC3/AIB1 is most important as it is amplified in breast cancers and forms a stable complex with estrogen receptor in breast cancer cells [Anzick et al., 1997; Tikkanen et al., 2000].

The p160 coactivators share a common domain structure, including a highly conserved N-terminal basic-helix-loop-helix (bHLH) and Per-Arnt-Sim (PAS) domains [Leo and Chen, 2000]. The PAS domain is separated into A and B regions, both are conserved across many PAS family proteins [Huang et al., 1993]. This bHLH-PAS domain is implicated in mediating protein–protein interaction. To investigate the mechanisms that regulate RAC3 activity, we have isolated several RAC3-interacting proteins through yeast two-hybrid screening. Recently, a novel family of ankyrin repeat-containing cofactors (ANCO-1 and ANCO-2) were also identified and shown to interact with p160 coactivators and HDACs, but not directly with NRs [Zhang et al., 2004]. Ectopic overexpression of ANCO-1 represses ligand-dependent transactivation by NRs, suggesting that ANCO-1 may inhibit ligand-dependent transcription by recruiting HDACs to the p160-NR complex. Furthermore, ANCO-1 was predominantly nuclear with apparent accumulation at specific nuclear domains [Zhang et al., 2004], suggesting that subcellular localization may be involved in regulating the corepressor activity of ANCO-1.

The transportation of large proteins (e.g., ANCO-1, 298 kDa) from the cytoplasm into nucleus requires an energy-dependent import mechanism (for reviews, see [Weis, 2003; Goldfarb et al., 2004]). One classic pathway for nuclear import is mediated by the importin α/β heterodimer. The most common NLSs are either mono-partite or bipartite. The mono-partite NLSs can be as long as 4 residues (pat 4) or 7 residues (pat 7), and are characterized by a cluster of positively charged lysine or arginine residues preceded by a helix-breaking residue such as proline. The bipartite NLS motifs consist of two clusters of basic residues separated by 9–12 residues. Recently, a ligand-activated NLS in the cellular retinoic acid binding protein-II (CRABP-II) was identified [Sessler and Noy, 2005]. While CRABP-II does not contain any predicted NLS in its primary sequence, such a motif was recognized in the protein's tertiary structure upon retinoic acid binding.

Proper localization to specific cellular compartments is vital for protein function. Nuclear proteins are transported into the nucleus in a highly regulated fashion, and delocalization can be associated with pathological conditions such as in leukemia [Dyck et al., 1994; Weis et al., 1994; Smith and Koopman, 2004]. In this study, we have investigated the regulatory signals that determine nucleocytoplasmic transportation of ANCO-1. Indirect immunofluorescence microscopy analyses revealed that four ANCO-1 fragments localizes exclusively in the nucleus. Multiple nuclear localization signals (NLSs) are predicted within these fragments. Site-directed mutational analyses reveal multiple functional NLSs. Intriguingly, disruption of a N-terminal NLS is sufficient to block nuclear import of the full-length ANCO-1. Furthermore, we have established an essential role of nuclear localization for the transcriptional corepressor activity of ANCO-1 upon PR-mediated transcriptional activation.

MATERIALS AND METHODS

Plasmids

All plasmids used in our laboratory are carefully documented in a database and identified with unique ID numbers, and confirmed by both enzyme restriction digestion and DNA sequencing. The pCMXHA-ANCO-1 expresses full-length wild-type ANCO-1 linked with an HA tag and a linker sequence (MDYPYDVPDYARA) to its N-terminus as previously described [Zhang et al., 2004]. The ANCO-1 ΔRD2 mutant was created by digesting pCMXHA-ANCO-1 with BamH*I* and Nhe*I*, followed by klenow "fill-in" reaction and self-ligation. This resulted in a C-terminal truncation at residue D2234 followed by two amino acid residues PS before a stop codon. Plasmid pCMXHA-RS13N (3–455) was obtained by PCR amplification directly from an EST clone (tf70e12, IMAGE# 2104654, GenBank #AI422295). Plasmid pCMXHA-RS13C (2369–2663) was derived from the original yeast two-hybrid clone pACT2-RS13C (2369–2663). Other pCMXHA-ANCO-1 constructs were generated by PCR reactions using pfu polymerase and their details are available upon request. The pEGFP-ANCO-1 NLS (74–90) and pEGFP-ANCO-1 NES (2410–2427) were generated by

direct subcloning of double-stranded oligonucleotides into the pEGFP-C1 vector (Clontech) at the Xho*I* and BamH*I* sites. The pCMXGalVP-ANCO-1 NES and pCMXGalVP-ANCO-1 NESm were made by subcloning a PCR-amplified VP16 AD (aa 413–490) fragment and respective double-stranded NES or NES mutant oligonucleotides into the pCMXGal-N vector at EcoR*I* and BamH*I* sites. The oligonucleotides for NLS are 5′-t cga gac aca gag aag cag ggc cct gag cgg aag agg att aag aag gag cct gtc tga g (sense) and 5′-ga tcc tca gac agg ctc ctt ctt aat cct ctt ccg ctc agg gcc ctg ctt ctc tgt gtc (antisense). The oligonucleotides for NES are 5′-t cga gtg atc cag cag acg ctg gcc gcc atc gtg gac gcc atc aag ctg gat gcc atc tga g (sense) and 5′-ga tcc tca gat ggc atc cag ctt gat ggc gtc cac gat ggc ggc cag cgt ctg ctg gat cac (antisense). The oligonucleotides for NESm are 5′-t cga gtg atc cag cag acg ccg gcc gcc acc gcg gac gcc acc aag ccg gat gcc atc tga g (sense) and 5′-ga tcc tca gat ggc atc cgg ctt ggt ggc gtc cgc ggt ggc ggc cgg cgt ctg ctg gat cac (antisense).

Site-Directed Mutagenesis and Primer Sequences

Site-directed mutagenesis was conducted using the QuikChange® site-directed mutagenesis kit (Stratagene). The sequences (5′ to 3′) of the sense primers used to generate indicated mutations are listed here: 82A, g cag ggc cct gag gcg gcg gcg att gcg gcg gag cct gtc acc cg; 456A, g gaa aaa aat aaa gtg aaa gcg gcg gca gcg gca gaa aca aaa gg; 593A, cg ctg aag cca gtg gcg gcg gcg cag gag cac agg; 630A, ggg aaa gtt gtc gca gca cat gca aca aaa cac; 765A, ctg tac aaa gag gag gca gcg gcg gca tca aaa gac cgg; 906A, gag ccc ttc ttc gca gcg gcg gac gcg gac tat ttg gat aaa aac; 919A, g gat aaa aac tct gag gcg gcg gca gag cag act gaa aag c; 939A, cg gaa aag gac gcg gcg gcg gca gag tcc gca gag; 2385A, g gcc cag cat ccg gcc gca gcc gcc ttt cag cgc tcc acc; 2415P, cag acg ccg gcc gcc acc gcg gac gcc acc aag ccg tag gct agc. The sequences of the antisense primers are antiparallel to the sense primers. All mutations were confirmed by DNA sequencing.

Cell Culture, Stable Cell Lines, and Transient Transfection

COS-7 and HEK293 cells were grown in Dulbecco's modified Eagle's medium, supplemented with 10% fetal bovine serum (FBS) and 5 μg/ml gentamycin (Gibco BRL, Carlsbad, CA). To generate ANCO-1 stable cell lines, HEK293 cells were transfected with pCMXHA-ANCO-1 together with a neomycin-resistant selection plasmid. Transfected cells were allowed to recover for 36 h before selecting with neomycin (G418, 1.5 mg/ml, Gibco). Neomycin-resistant colonies derived from single cells were selected and grown in neomycin-containing media.

For transient transfection, COS-7 cells were seeded in 12-well plates and transfected 24 h later with 2.5 μg of plasmid DNA per well by standard calcium phosphate precipitation method. Cells were incubated with DNA precipitates for approximately 12 h, and precipitates were subsequently removed by washing with phosphate buffered saline (PBS) containing calcium and magnesium. Cells were cultured for additional 48 h, after which cells were harvested and analyzed for luciferase and β-galactosidase activity.

Immunofluorescence Microscopy

COS-7 cells were grown on cover glass in 24-well plates and transfections were conducted as described above. After transfection, cells were incubated for another 24–36 h before fixation with cold methanol/acetone (1:1) mixture for 2 min. The fixed cells were then processed for immunofluorescence staining as previously described [Dyck et al., 1994]. Briefly, the fixed cells were incubated with primary antibodies followed by rhodamine- or fluorescein-conjugated secondary antibodies. Cell nuclei were counterstained with DAPI (4′,6-diamidino-2 phenylindole) and cover glasses were mounted with Pro-Long anti-fade reagents (Molecular Probe). The images were visualized with a Zeiss Axiovert 200 microscope equipped with an Axiocam and Axiovision software (Zeiss). The mouse anti-HA monoclonal (Santa Cruz Biotechnology, Inc.), rabbit anti-HA polyclonal (Medical Biological Lab, Inc.), and mouse anti-Gal4 DBD monoclonal (Calbiochem, Inc.) antibodies were obtained from indicated commercial sources. The anti-ANCO-1 monoclonal antibody was generated against a mixture of GST-ANCO-1 fragments (GeneTex, Inc.).

RESULTS

ANCO-1 Localizes at Discrete Nuclear Domains

We have shown that transiently transfected ANCO-1 localizes in nuclear dot-like structures [Zhang et al., 2004]. To further investigate the mechanisms that determine subnuclear

localization of ANCO-1, we generated a mouse anti-ANCO-1 monoclonal antibody and analyzed localization of endogenous and stably transfected ANCO-1. The ANCO-1 antibody specifically recognized the transfected HA-ANCO-1, whereas preimmune serum did not (Fig. 1A). In non-transfected cells, the ANCO-1 antibody also detected endogenous nuclear dot structures, whereas preimmune serum did not (Fig. 1B), suggesting that endogenous ANCO-1

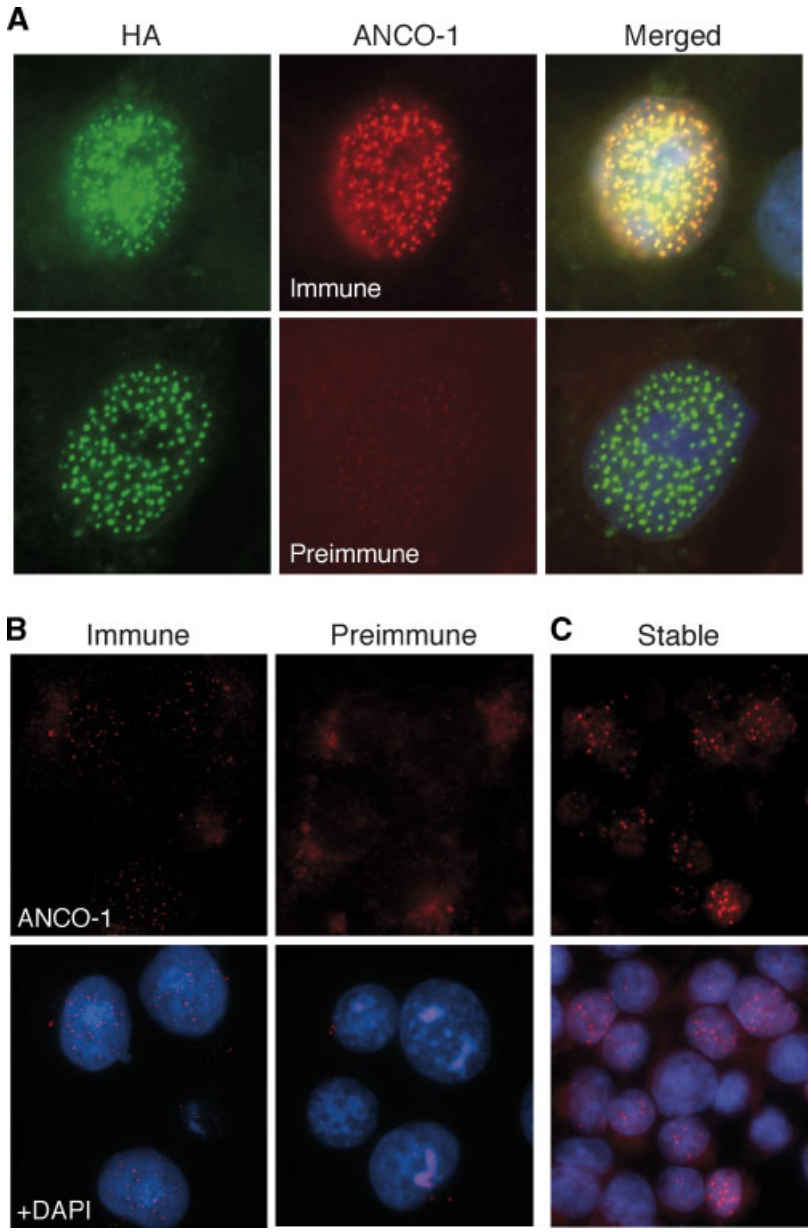

Fig. 1. Localization of ANCO-1 at discrete nuclear domains. **A**: Mouse anti-ANCO-1 antibody detects HA-ANCO-1. COS-7 cells were transiently transfected with HA-ANCO-1 expression vector, following by immunofluorescence staining using rabbit anti-HA polyclonal antibody and mouse anti-ANCO-1 monoclonal antibody. The rabbit primary antibody was detected with FITC (green)-conjugated goat anti-rabbit IgG secondary antibody; while the mouse primary antibody was detected with Rhodamine (red)-conjugated goat anti-mouse IgG secondary antibody. A transfected cell shows precise overlap of the FITG- and rhodamine-stained dots in the nucleus. The preimmune serum did not show any staining of the HA-ANCO-1. **B**: ANCO-1 monoclonal antibody detects endogenous nuclear dots. Non-transfected COS-7 cells were immunostained with mouse anti-ANCO-1 antibodies. Specific nuclear dots were detected at endogenous levels. The preimmune serum shows no staining of nuclear dots. **C**: Formation of ANCO-1 nuclear dots in HA-ANCO-1 stably transfected HEK293 cells. More than 50% of cells in this stable clone are positive for ANCO-1 staining, and all positive cells exhibit nuclear dots staining. [Color figure can be viewed in the online issue, which is available at www.interscience.wiley.com.]

is also localized at discrete nuclear bodies. We refer to these nuclear structures as "ANCO-1 bodies." In support of this idea, we generated stable HEK293 cell lines containing a HA-ANCO-1 expression vector and observed similar structures with both anti-HA (Fig. 1C) and ANCO-1 antibody (not shown). These results indicate that ANCO-1 indeed localizes at discrete nuclear domains under steady-state conditions.

Localization of ANCO-1 Fragments

To understand the mechanisms by which ANCO-1 is localized in the nucleus at ANCO-1 bodies, we analyzed the distribution of a series of ANCO-1 fragments trying to locate regions that may contain targeting sequences (Fig. 2A). These ANCO-1 fragments contain HA epitopes at N-termini, were transiently transfected into culture cells, and analyzed by immunofluorescence microscopy using anti-HA antibodies (Fig. 2B). In this assay, the following fragments were found localized in the nucleus: *a* (1–127), *b* (3–455), *d* (318–611), *e* (611–948), and *k* (2369–2663), suggesting that these regions may contain NLS sequences. The other fragments were localized all over the cells or in the cytoplasm, suggesting that they lack nuclear import or contain nuclear export signals (NESs). Among these nuclear fragments, fragments *e* and *k* also formed dot-like structures, while fragments *a*, *b*, and *d* were distributed homogenously in the nucleus. These results suggest that subcellular localization of ANCO-1 may be regulated by multiple signals at different regions.

Identification of Nuclear Localization Signals in ANCO-1

ANCO-1 is predicted as a nuclear protein with 94% reliability using Reinhardt's method for cytoplasmic/nuclear discrimination. Indeed, multiple putative NLSs could be predicted throughout the entire ANCO-1 sequence using computer algorithms. Visual inspections of these NLSs excluded several overlapping sequences, reducing putative NLSs to 17 sites (Fig. S1A, Supplementary Material). Among these 17 sites, only 8 were actually located within ANCO-1 nuclear fragments (Fig. S1B, Supplementary Material). To determine which of these eight candidate NLSs are actually responsible for nuclear import of ANCO-1, we mutated all eight sites individually or combinatorially in the context of the four ANCO-1 nuclear fragments, *a*, *d*, *e*, and *k*, hopefully avoiding redundant NLSs. In the N-terminus a (1–127) fragment, only one NLS was predicted at residues 80–87. Interestingly, replacing residues 80–87 from PERKRIKK to PEAAAIAA (82A mutation) completely abolished nuclear localization of the *a* fragment (Fig. 3), suggesting that residues 80–87 constitute a functional NLS (designated as NLS1). Similarly, the C-terminus *k* (2369–2663) fragment also contains only one candidate NLS at residues 2384–2390. We replaced this sequence from PRKRRFQ to PAAAAFQ (2385A mutation) and found it also completely abolished nuclear localization of this C-terminal fragment (Fig. 3), suggesting that residual 2384–2390 also constitute a functional NLS (designated as NLS2). We noticed that the 82A mutation caused diffuse cytoplasmic localization, while the 2385A mutation caused accumulation outside of nuclear envelope, suggesting distinct mechanisms of nuclear transportation mediated by these two NLSs.

Attempts to test the predicted NLSs within *d* and *e* fragments were also performed. There are two predicted NLSs within the *d* fragment (Fig. S1B, Supplementary Material). Replacing the first sequence at residues 455–475 from KKKRKKETKGREVRFGKRSDK to KAAAAAETKGREVRFGKRSDK (456A mutation) had little or no effect on nuclear localization of this fragment. Similarly, replacing the second sequence at residues 591–597 from PVRKRQE to PVAAAQE (593A mutation) also had little or no effect. Surprisingly, introduction of both 456A and 593A mutations completely abolished nuclear translocation of this fragment, suggesting that these two sites may be redundant in mediating nuclear import of the *d* fragment.

Extensive mutational analyses were also performed to test candidate NLSs responsible for nuclear localization of the *e* (611–948) fragment. Within this region, four putative NLSs were predicted, including three pat4 NLSs at residues 630–633, 765–768, and 939–942, and a bipartite NLS at residues 903–923 (Fig. S1, Supplementary Material). Replacing the bipartite sequence at residues 903–923 from PFFRKKDRDYLDKNSEKRKEQ to PFFAAADADYLDKNSEKRKEQ (906A mutation), PFFRKKDRDYLDKNSEAAAEQ (919A mutation), or in combination to PFFAAADADYLDKNSEAAAEQ (906A/919A mutation) had no effect on nuclear localization of this fragment (data not shown), suggesting

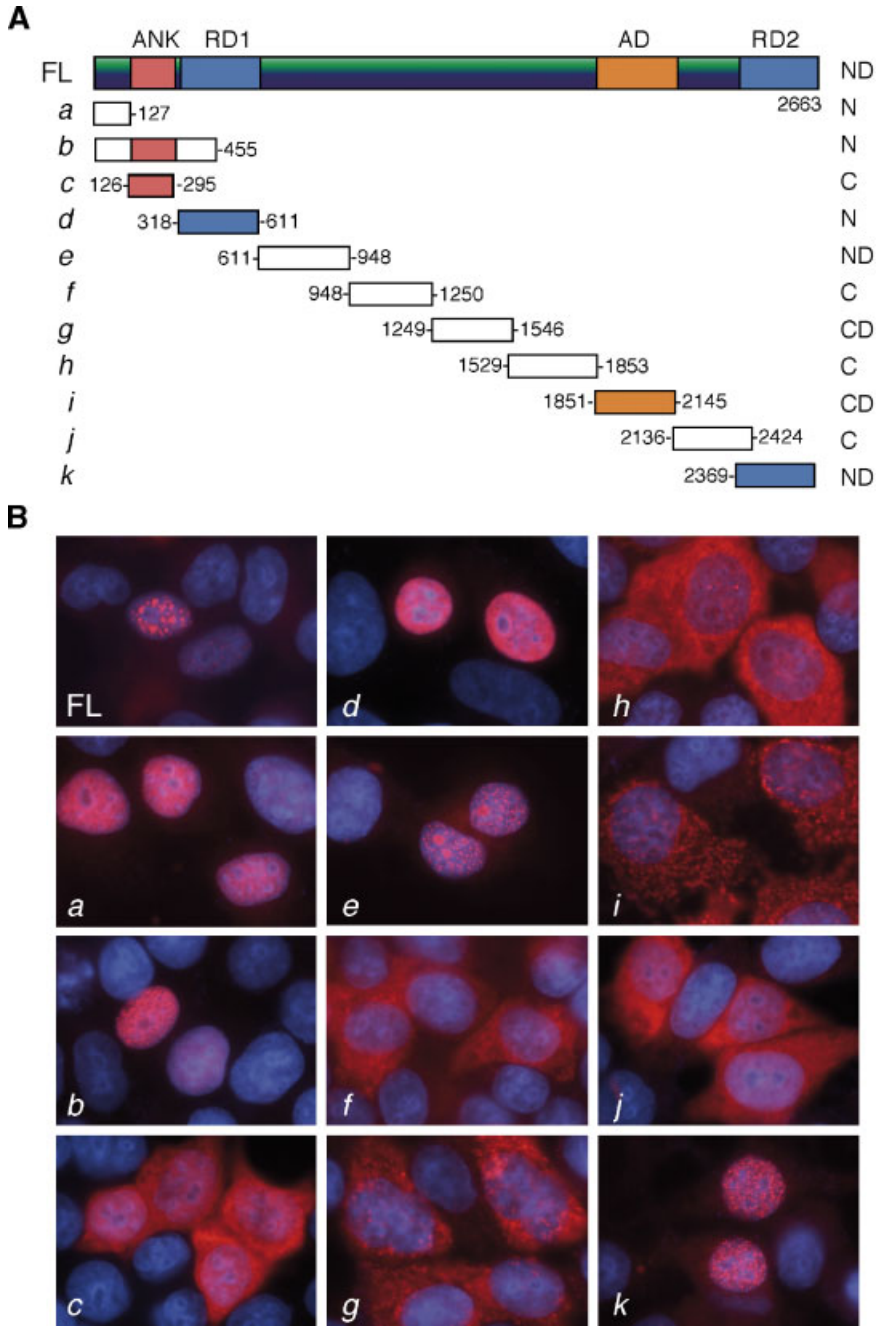

Fig. 2. Subcellular localization of ANCO-1 fragments. **A**: Schematic diagram of HA-ANCO-1 fragments. Structural domains are marked on top: ANK, ankyrin repeats; RD1, repression domain 1; AD, activation domain; RD2, repression domain 2. The starting and ending amino acid residues of each fragment are next the fragment. The localization patterns of these fragments are summarized at the right. N, nuclear; ND, nuclear dots; C, cytoplasmic, CD, cytoplasmic dots. **B**: Representative images showing localization of each ANCO-1 fragment. COS-7 cells were transiently transfected with indicated fragments (FL, full-length ANCO-1 or fragments *a*–*k*), followed by indirect immunofluorescence analyses using an anti-HA monoclonal antibody and rhodamine-conjugated secondary antibody (red). Cell nuclei were stained with DAPI (*4,6*-diamidino-*2*-phenylindole). The merged images of rhodamine and DAPI signals are shown. [Color figure can be viewed in the online issue, which is available at www.interscience.wiley.com.]

that residues 903–923 is not involved in nuclear localization. Other combinatorial mutations replaced residues 630–633 from KKHK to AAHA (630A mutation), residues 765–768 from RKKK to AAAA (765A mutation), or residues 939–942 from KKRR to AAAA (939A mutation), in combination with 906A or 919A mutation, creating 906A/630A, 906A/765A, 906A/939A,

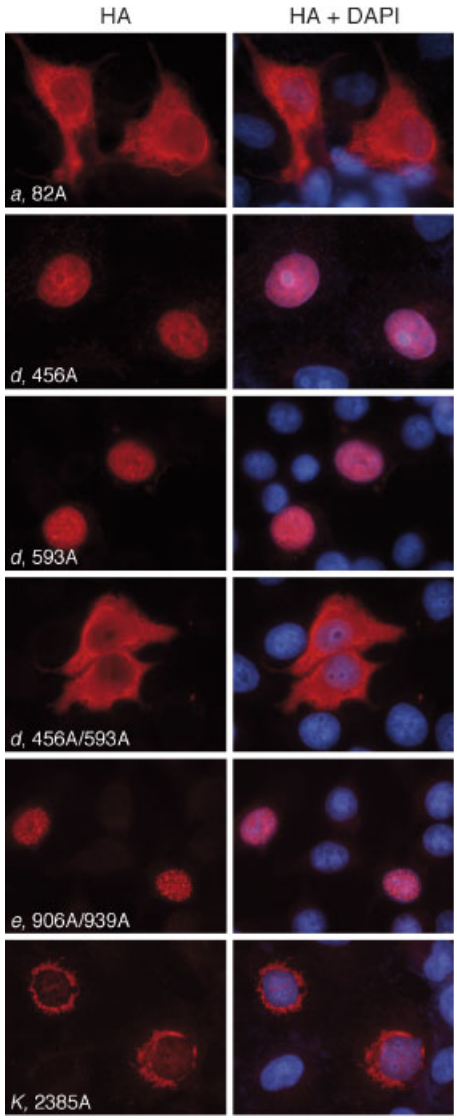

Fig. 3. Mutational analyses of putative ANCO-1 NLSs. Localization of ANCO-1 NLS mutants. COS-7 cells were transiently transfected with indicated plasmids encoding various NLS mutations in ANCO-1 fragments *a, d, e,* or *k*. Transfected cells were analyzed by indirect immunofluorescence using an anti-HA monoclonal antibody (red) and DAPI to delineate nuclei. [Color figure can be viewed in the online issue, which is available at www.interscience.wiley.com.]

and 919A/630A double mutants. None of these mutations had any apparent effects on nuclear localization of this fragment (Fig. 3 and data not shown). Therefore, the mechanisms mediating nuclear localization of this 611–948 fragment may be distinct from the traditional pathways.

NLS1 Determines Nuclear Localization of Full-Length ANCO-1

To determine the relative contributions of different functional NLSs in ANCO-1 on nuclear localization of the full-length protein, we created NLS mutations in the context of full-length ANCO-1 (Fig. 4A). When the 82A/NLS1 mutation was introduced, we surprisingly found that it alone was able to completely disrupt nuclear import of full-length ANCO-1 (Fig. 4B). In contrast, the 2385A/NLS2 mutation alone had no effect on nuclear localization of the full-length protein. As expected, the double mutant 82A/2385A showed complete cytoplasmic distribution as the 82A mutant. These data suggest that the N-terminal NLS1 at residues 80–86 is most crucial for nuclear import of full-length ANCO-1, while the C-terminal NLS2 at residues 2384–2390 may be dispensable in the presence of NLS1 in

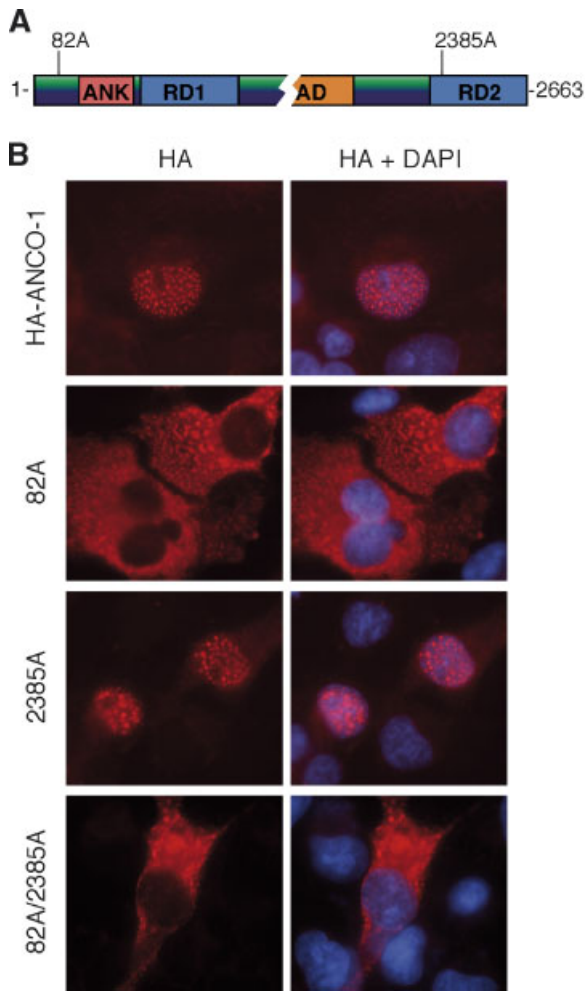

Fig. 4. A: Schematic representation of the full-length ANCO-1 and positions of the 82A and 2385A NLS mutations. B: Localization of full-length ANCO-1 NLS mutants. [Color figure can be viewed in the online issue, which is available at www.interscience.wiley.com.]

full-length protein. Since mutation of NLS1 is sufficient to disrupt nuclear localization of full-length ANCO-1, it suggests that other potential NLSs at central region of the protein, such as the NLSs at residues 455–475 and 591–597, may not be functional in the context of full-length protein. Therefore, we have not further analyzed their effects on nuclear localization of the full-length ANCO-1.

ANCO-1 Contains a Putative Nuclear Export Signal

In addition to nuclear import, protein localization is also regulated by nuclear export mostly through a CRM1-dependent, leptomycin B (LMB)-sensitive mechanism [Fukuda et al., 1997]. To determine if nuclear export also plays a role in regulating ANCO-1 localization, we searched for potential NES consensus sequences within ANCO-1 fragments localized in the cytoplasm. Interestingly, we found that fragment *j* (aa 2136–2424) contains a leucine-rich NES consensus sequence at residues 2415–2424 (Fig. 5A). This putative NES sequence, LAAIVDAIKL, is highly conserved among known NESs in other proteins (Fig. 5B). To test whether this motif is indeed a functional NES, we treated cells with LMB to block CRM1 activity and determined the effects on localization of fragment *j*. Consistently, fragment *j* was localized almost exclusively in the cytoplasm in the absence of LMB treatment (Fig. 5C), while LMB caused accumulation of this fragment in the nucleus. We also tested the effects of LMB on distributions of other ANCO-1 cytoplasmic fragments and found little or not effect (data not shown). To directly test whether the putative NES sequence indeed mediates ANCO-1 nuclear export, we mutated residues 2415–2424 from LAAIVDAIKL to PAATADATKP (Fig. 5B, 2415P mutation). This mutation is expected to disrupt the conserved hydrophobic residues that are essential for NES activity of other proteins [Fukuda et al., 1997]. Remarkably, the 2415P mutation caused significant accumulation of fragment *j* in the nucleus. Therefore, we have identified a functional NES that mediates nuclear export of ANCO-1 through a CRM1-dependent pathway.

NLS1 and NES of ANCO-1 Act Autonomously to Mediate Protein Localization

To corroborate the findings of NLS and NES of ANCO-1, we determine if the NLS and NES sequences could act autonomously to mediate localization of heterologous proteins. We fused the NLS1 sequence of residues 74–90 and the NES sequence of residues 2410–2427 to the C-terminus of EGFP (Fig. 6A). The NLS1 and NES sequence were linked to EGFP aa 1–239 through a spacer SGLRSR sequence, and a random sequence encoded by the polylinker sequence of the pEGFP-C1 vector served as a negative control. We found that the EGFP protein distributed uniformly throughout the cell, while the EGFP-NLS1 localized primarily in the nucleus (Fig. 6B). In contrast, the EGFP-NES fusion showed exclusive cytoplasmic staining. These results suggest that both NLS1 and NES motifs of ANCO-1 are sufficient to mediate nuclear import and export of heterologous protein, respectively.

ANCO-1 NES Inhibits Transcriptional Activity of GalVP

To determine if the NES sequence of ANCO-1 could also alter activity of heterologous proteins, we tested its ability to regulate the transcriptional activity of the chimeric Gal4 DBD-VP16 AD fusion protein (GalVP). The wild-type NES sequence at residues 2410–2427 and the mutant sequence (NESm) with 2415P mutation were linked to the C-terminus of GalVP (Fig. 7A). The effects of NES and NESm on GalVP-mediated transactivation of a Gal4-dependent luciferase reporter were determined by transient transfection in COS-7 cells (Fig. 7B). We found that the wild-type GalVP activated the reporter strongly (over 100-fold). In contrast, GalVP-NES showed reduced transcriptional activity ($P < 0.05$), while GalVP-NESm had no effect on GalVP activity. These results suggest that the NES sequence can inhibit transcriptional activity of a transcription factor.

To determine if the NES-mediated inhibition of GalVP transcriptional activity indeed correlates with nuclear export, subcellular distributions of GalVP, GalVP-NES and GalVP-NESm were analyzed by immunofluorescence microscopy (Fig. 7C). The wild-type GalVP was localized exclusively in the nucleus, due to an NLS in the Gal4 DBD. In contrast, the GalVP-NES localized mainly in the cytoplasm, consistent with its nuclear export activity. As expected, the GalVP-NESm remained in the nucleus, indicating that the 2415P mutation disrupts the NES function. The ability of

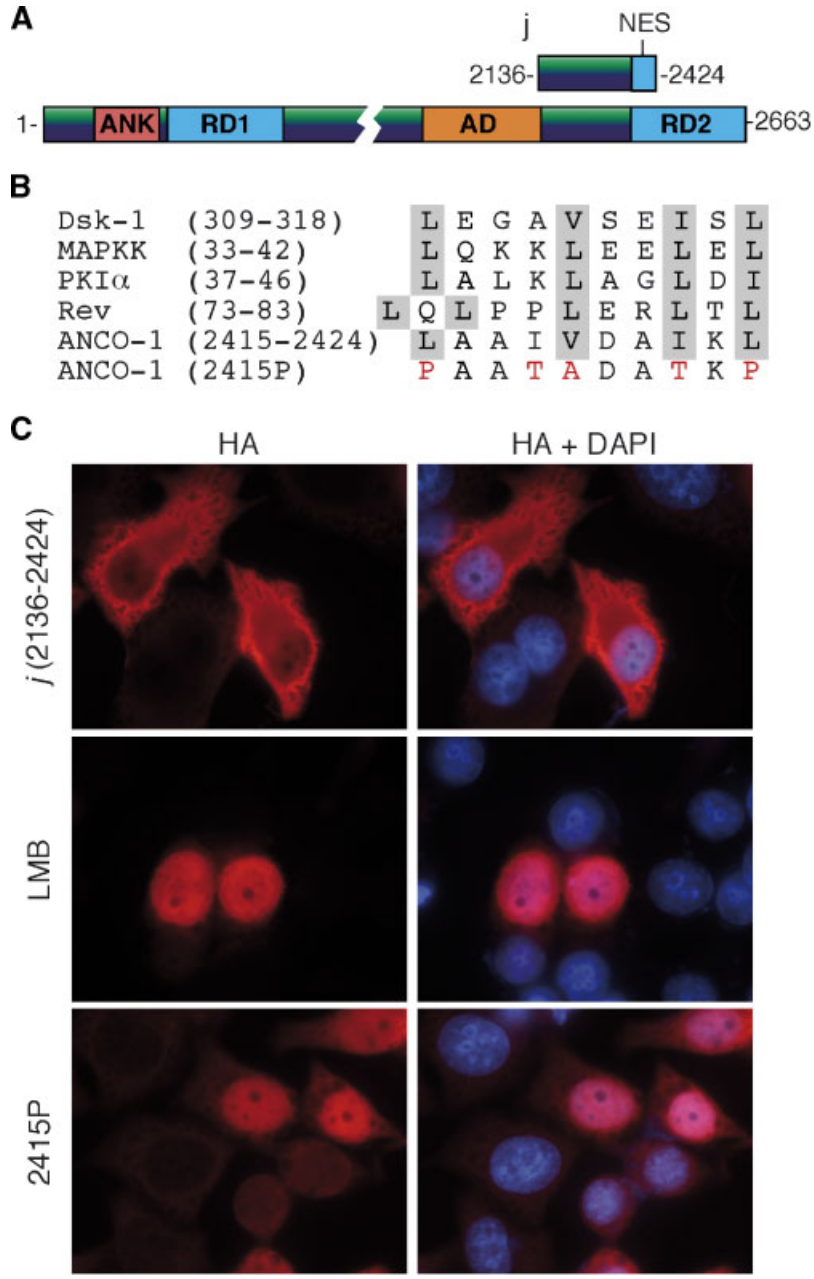

Fig. 5. Identification of a nuclear export signal of ANCO-1. **A**: Schematic representation of the position of the ANCO-1 NES and the NES-containing fragment (aa 2136–2424). **B**: Alignment of the predicted leucine-rich nuclear export signal (NES) of ANCO-1 (aa 2415–2424) with known NES sequences. The ANCO-1 NES mutant (NESm, 2415P) sequence is shown at the bottom, with mutated residues in red. The shaded residues are conserved hydrophobic residues essential for NES function in the other proteins. **C**: Leptomycin B (LMB) and 2415P mutation (NESm) block cytoplasmic export of the ANCO-1 fragment. COS-7 cells were transiently transfected with indicated constructs and the transfected cells were treated with LMB (1 μM) or solvent for 12 h. Cells were fixed and stained with anti-HA antibody and rhodamine-conjugated secondary antibody (red). The wild-type ANCO-1 fragment is located in the cytoplasm, and LMB treatment causes its accumulation in the nucleus. The NESm (2415P) mutant is localized mainly in the nucleus. [Color figure can be viewed in the online issue, which is available at www.interscience.wiley.com.]

GalVP-NES to partially activate transcription (Fig. 7B) may be due to transient nuclear localization before exportation to the cytoplasm. These results correlate precisely with the reporter assay, demonstrating that the ANCO-1 NES is capable of mediating nuclear export of GalVP, resulting in inhibition of its transcriptional activity in the nucleus.

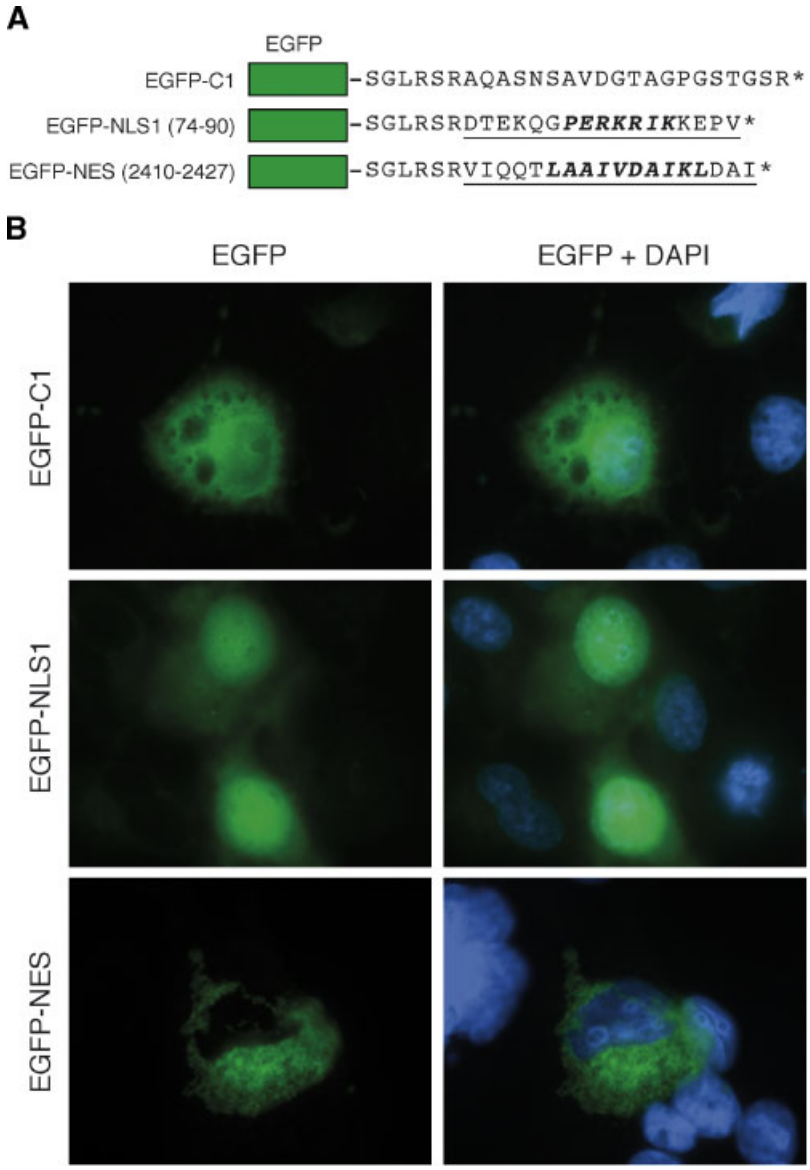

Fig. 6. NLS and NES sequences of ANCO-1 act autonomously to mediate localization of heterologous protein. **A**: Schematic diagram of wild-type EGFP, EGFP-NLS1 (74–90), and EGFP-NES (2410–2427) fusion constructs. The sequences after residue 239 of EGFP are shown. Underlined residues are the NLS (aa 74–90) and NES (aa 2410–2427) sequences of ANCO-1. Boldfaced italic residues are the canonical NLS and NES consensus sequences, respectively. **B**: Localization of the EGFP, EGFP-NLS1, and EGFP-NES fusions. COS-7 cells were transiently transfected with respective constructs and were allowed to recover for 24 h after transfection. Transfected cells were fixed in 4% paraformaldehyde and counter stained with DAPI for nuclei (blue). [Color figure can be viewed in the online issue, which is available at www.interscience.wiley.com.]

Nuclear Localization Is Required for Corepressor Activity of ANCO-1

We have previously shown that overexpression of ANCO-1 inhibits NR-mediated transcriptional activation [Zhang et al., 2004], which occurs presumably in the nucleus. Since the 82A/NLS1 mutation disrupts nuclear localization of full-length ANCO-1 (Fig. 4), it provides a tool to test whether nuclear localization is required for the corepressor activity of ANCO-1. We analyzed the activities of full-length ANCO-1 and mutants on progesterone receptor (PR)-mediated transcriptional activation by reporter gene assay (Fig. 8). In the absence of ligand, ANCO-1 and mutants had no effect on basal promoter activity. Progesterone stimulated PR transactivation of the MMTV reporter strongly. Consistently, coexpression of wild-type ANCO-1 led to a significant about 50%

reduction on PR activity. Interestingly, this inhibitory effect was abolished in the 82A/NLS1 mutant, suggesting that nuclear localization is important for the transcriptional corepressor activity of ANCO-1. In contrast, the NES 2415P mutant of full-length ANCO-1, which had no effect on nuclear localization of the full-length protein (data not shown), was still capable of inhibiting PR-mediated transcriptional activation. Similarly, the silent 2385A/NLS2 mutation also had no effect on the corepressor activity of ANCO-1. These results suggest that the NLS1 motif and nuclear localization are important for the nuclear corepressor function of ANCO-1.

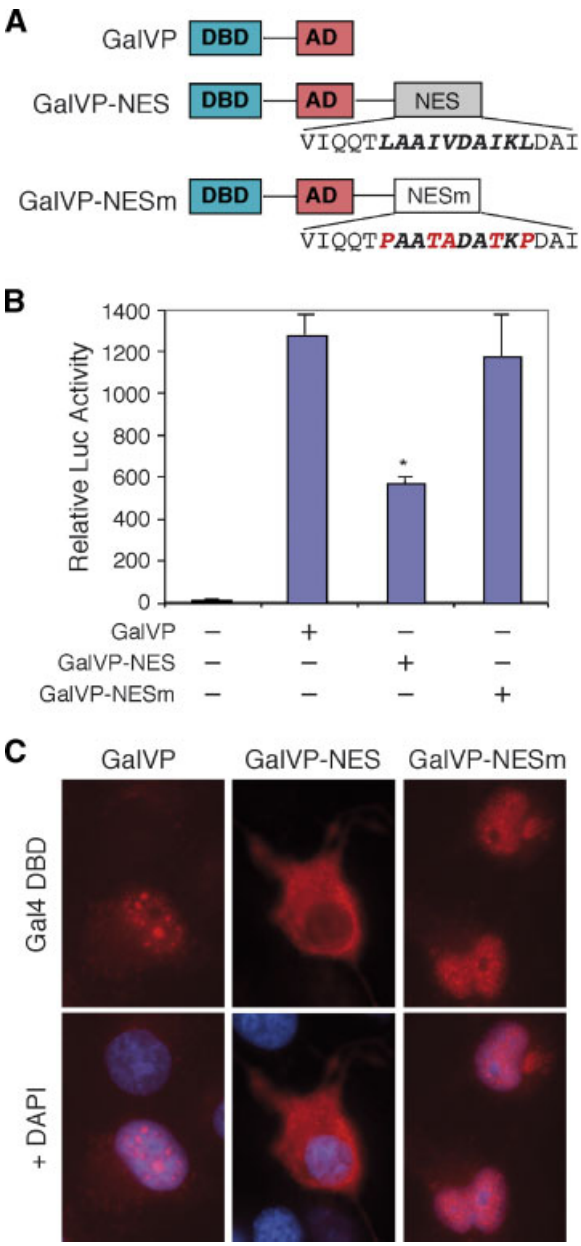

DISCUSSION

We previously identified ANCO-1 as a novel ankyrin repeats nuclear protein implicated in regulating NR transcriptional activity through physical association with coactivators and corepressors [Zhang et al., 2004]. ANCO-1 is also implicated in nasopharyngeal carcinoma and childhood medulloblastoma [Behrends et al., 2003], and the gene is located at a region (16q24.3) frequently deleted in cancer [Powell et al., 2002; Behrends et al., 2003]. One interesting feature of ANCO-1 is its localization at discrete subnuclear domains, termed ANCO-1 bodies. ANCO-1 bodies may represent novel nuclear structures because so far they do not overlap with known structures such as PML bodies, SC35 splicing speckles, or interphase centromeres [Zhang et al., 2004]. Here, we report the observation of ANCO-1 bodies at endogenous levels and stably transfected cells (Fig. 1), confirming that ANCO-1 is indeed a nuclear protein concentrated at discrete subnuclear compartments. We further identify both nuclear localization (NLS) and nuclear export (NES) signals within ANCO-1, and establish that nuclear localization is essential for the corepressor activity of ANCO-1. We reveal an N-terminal NLS at residues 80–86 (NLS1), and show that its mutation alone is sufficient to block nuclear import of full-length ANCO-1. A second NLS (NLS2)

Fig. 7. The NES sequence of ANCO-1 inhibits nuclear localization and transcriptional activity of Gal4-VP16 fusion. **A**: Schematic representation of the Gal4 DBD (aa 1–147)-VP16 AD (aa 413–490) fusion, GalVP-NES, and GalVP-NESm. The NES and NESm sequences, corresponding to aa 2410–2427 of ANCO-1, are linked to the C-terminus of GalVP. Boldfaced italic residues indicate the canonical NES motif. Mutated residues of the NESm are shown in red. **B**: Transcriptional activities of GalVP-NES and mutant. COS-7 cells were transfected with indicated constructs together with a Gal4-dependent luciferase reporter MH100-tk-Luc and a β-Galactosidase internal control. Relative luciferase activities were determined from three independent transfections after normalization to β-galactosidase activities. The transcriptional activity of GalVP-NES is significantly lower ($^*P < 0.01$) than GalVP and GalVP-NESm. **C**: Immunofluorescence analysis shows localizations of GalVP, GalVP-NES, and GalVP-NESm. COS-7 cells were transiently transfected with indicated constructs and the transfected cells were stained with an anti-Gal4 DBD monoclonal antibody and DAPI for nuclei. [Color figure can be viewed in the online issue, which is available at www.interscience.wiley.com.]

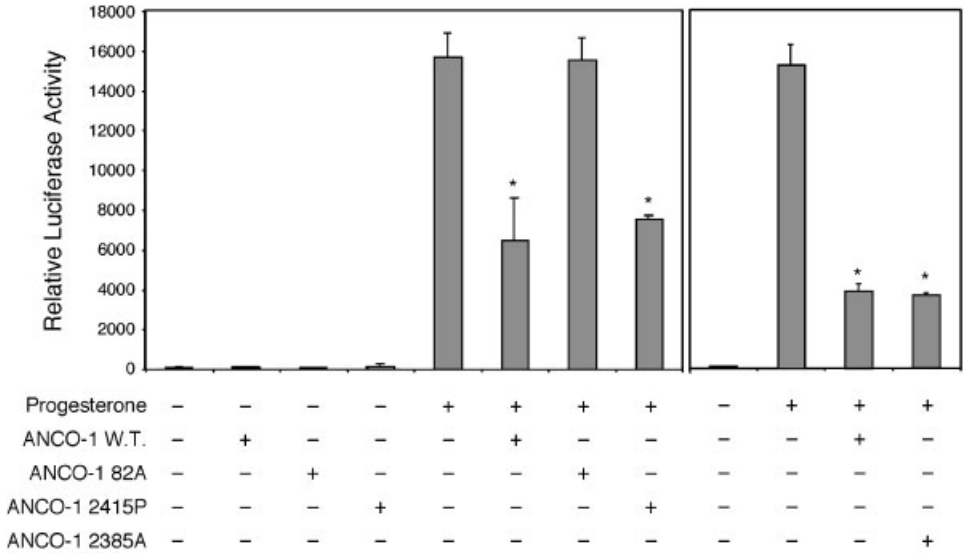

Fig. 8. Nuclear localization is essential for corepressor activity of ANCO-1. COS-7 cells were transiently transfected with hPR-B expression vector, MMTV-Luc reporter, β-galactosidase control, together with indicated ANCO-1 constructs. Transfected cells were treated with or without progesterone at 0.1 nM to activate reporter gene expression. Relative luciferase activities were determined from three independent transfections after normalization with β-galactosidase control. Wild-type ANCO-1 diminishes PR-mediated transactivation as well as the ANCO-1 NESm and 2385A mutants (*$P < 0.01$). The 82A NLS mutant of ANCO-1 lost the transcriptional inhibitory activity. Statistical analyses were performed using one-way ANOVA followed by Tukey HSD test.

is found at residues 2384–2390, but it is only required to mediate nuclear import of a C-terminal fragment and not the full-length protein. In addition, we also identify a NES at residues 2415–2424 and show that it can inhibit transcriptional activity of a chimeric transcription factor. Furthermore, we show that both NLS1 and NES of ANCO-1 can act autonomously to mediate nuclear import and export of heterologous proteins, respectively. Finally, a correlation between nuclear localization of full-length ANCO-1 and its corepressor activity is established.

In an attempt to decipher the regulatory mechanisms controlling ANCO-1 nuclear distribution pattern and its corepressor function, we used Reinhardt's NLS prediction program to locate potential NLS sequences within ANCO-1. Many putative NLSs were identified. These are either short stretches of 4 (pat 4) or 7 (pat 7) basic residues of the mono-partite category that are usually preceded by a helix-breaking residue such as proline, or the more complex bipartite signals consisted of two clusters of basic residues separated by 9–12 residues. Experimentally, we have compared the localization of a series of ANCO-1 fragments, spanning the entire protein, and identified four ANCO-1 fragments that are localized in the nucleus. These four nuclear fragments contain a total of eight predicted NLS sequences. The N-terminal nuclear fragment (aa 1–127) and the C-terminal nuclear fragment (aa 2369–2663) each contains only a single predicted pat7 NLS between residues 80–86 (PERKRIK, NLS1) and 2384–2390 (PRKRRFQ, NLS2), respectively. Mutations of basic residues within these two motifs into alanines completely abolished nuclear localizations of respective fragments (Fig. 3), suggesting that these are two functional NLSs of ANCO-1.

Our attempts to locate NLS sequences in the central 318–611 and 611–948 fragments were less successful, partly due to the multiplicity of the potential NLS sequences located within these two fragments. In the 318–611 fragment, there are two clusters of basic residues at aa 455–475 (KKKRKKETKGREVRFGKRSDK, underlined residues are mutated to alanines in the 456A mutation) and aa 591–601 (PVRKRQEHRKR, underlined residues are mutated to alanine in the 593A mutation). The sequence of the first cluster contains two potential configurations for a bipartite NLS and three potential configurations for a pat 4 NLS. Mutation of the 5 consecutive basic residues starting at residue 456 into alanines (456A) had no effect on nuclear localization

of this fragment. We expected that the 456A mutation would have disrupted all three potential pat4 NLS configurations, as well as the N-terminal basic residues of the two potential configurations of a bipartite NLS. Nevertheless, the 456A mutation does not affect the C-terminal basic residues for the predicted bipartite NLSs. Therefore, whether this cluster of basic residues contains any functional NLS remains to be determined. Similarly, the 591–601 cluster of basic residues contains one potential pat 7 NLS starting at residue 591 and one potential pat 4 NLS starting at residue 598. The 593A mutation affects only the pat 7 NLS, but not the pat 4 NLS. Therefore, again we are not certain whether the 593A mutation had eliminated all NLS activity at this region. However, a double 456A/593A mutation appears to disrupt nuclear localization. Therefore, it is possible that nuclear localization of this fragment might be determined by a non-classical NLS sequence(s) or that a NLS may be formed from different regions of the protein.

Multiple NLSs are also predicted within the 611–948 nuclear fragment of ANCO-1, including three potential pat 4 NLSs at residues 630 (KKHK), 765 (RKKK), and 939 (KKRR), one putative pat 7 NLS at residue 903, which happens to overlap with two possible configurations of a bipartite NLS starting at either residue 906 or 907 (aa 903–923, PFF-RKKDRDYLDKNSEKRKEQ, the first two underlined stretches of basic residues are mutated in 906A, the last underlined stretch of three basic residues are mutated in 919A). We have mutated each of these putative NLSs either singularly or in various combinations, but none of these mutations affected nuclear localization of this ANCO-1 fragment. For instance the 906A/919A double mutation should have completely disrupted the bipartite NLS, but the fragment remains in the nucleus. Similarly, mutation of the each of the pat 4 NLSs had no detectable effects on nuclear localization. Therefore, it appears that either all these predicted NLSs were functional and individually sufficient to mediate nuclear localization, or that there might be a certain unrecognized mechanism for nuclear import of this nuclear fragment. In additional to the existence of potential non-classical NLS or a NLS recognizable only by a three-dimensional structure; it is also possible that this domain might interact with other nuclear proteins to form a complex that could be translocated into nucleus via NLS sequences present on interacting proteins. Indeed, our preliminary data suggests that this 611–948 fragment could colocalize with the full-length ANCO-1 (data not shown), supporting the idea that this fragment may enter into nucleus by forming a complex with the full-length ANCO-1.

All in all, we were able to confirm two functional NLSs in this study, despite the prediction of over a dozen of NLSs within ANCO-1. One interesting phenomenon of the two identified NLSs is that they are not functionally equivalent in mediating nuclear import of the full-length ANCO-1. The 82A mutation of full-length ANCO-1 completely abolished nuclear localization, while the 2385A mutation had little or no effect (Fig. 4). The functionality of the N-terminal NLS1 was further demonstrated by the nuclear transport of the EGFP fused with this NLS motif. Furthermore, preliminary data revealed binding of an importin alpha molecule to the N-terminal domain of ANCO-1 (data not shown), suggesting an involvement of importin alpha in the nuclear transport of ANCO-1. It is likely that the C-terminal NLS is functional only in the context of an isolated fragment, whereas this NLS may be masked intramolecularly within the full-length ANCO-1 and becomes inaccessible to nuclear import machinery. One interesting example of intramolecular masking of the NLS is found in the NF-κB p105 precursor where the ankyrin repeat-containing C-terminus masks its NLS at the N-terminus [Henkel et al., 1992]. Whether the ankyrin repeat-containing N-terminus of ANCO-1 plays a role in masking the C-terminal NLS remains to be tested.

In addition to the elucidated functional NLSs, we have also identified a functional NES sequence within ANCO-1. Unlike stably transfected cells, transient transfection of ANCO-1 causes cytoplasmic distribution of the protein in a significant portion of the transfected cells. Upon examination of the sequences in the ANCO-1 cytoplasmic fragments, we identified a leucine-rich, short amino-acid sequence (LAAIVDAIKL) at amino acids 2415–2424, which is reminiscent of a classical NES [Fukuda et al., 1997; Kutay and Guttinger, 2005]. Indeed, the ANCO-1 fragment containing this putative NES is readily retained in the cytoplasm. Several lines of evidence support that

this NES of ANCO-1 is functional. First, LMB treatment causes nuclear accumulation of the ANCO-1 (2136–2424) fragment that contains the NES (Fig. 5). LMB is known to covalently modify and inactivate CRM1/exportin 1, which is responsible for nuclear export mediated by the classical NES [Fukuda et al., 1997; Kudo et al., 1999]. Secondly, mutation of the NES consensus residues also causes nuclear accumulation of this ANCO-1 fragment (Fig. 5). Furthermore, this NES sequence is sufficient to mediate cytoplasmic accumulation of heterologous proteins including EGFP and GalVP (Figs. 6, 7). Finally, the NES-mediated nuclear export of GalVP leads to inhibition of GalVP's transcriptional activity in the nucleus. Together, these results strongly suggest that ANCO-1 contains at least one functional NES.

Finally, we have also demonstrated the relevance of the above-identified ANCO-1 NLS and NES sequences in regulating transcriptional corepressor activity of ANCO-1. We have previously shown that wild-type ANCO-1 inhibits PR transcriptional activity [Zhang et al., 2004], whereas the NLS mutant failed to do so (Fig. 8). This finding suggests that nuclear localization is essential for ANCO-1 to regulate transcription. Since ANCO-1 exerts its transcriptional inhibitory activity through direct interaction with p160 coactivators and direct recruitment of HDACs to coactivator-NR complexes [Zhang et al., 2004], it is conceivable that such activity requires the presence of ANCO-1 in the nucleus. In contrast to the NLS mutant, the NES and 2385A mutants do not have any effect on the transcriptional inhibitory function of ANCO-1. Taken together, our data strongly suggest that nuclear import of ANCO-1 is essential for its transcriptional inhibitory activity. The insights found regarding nuclear import and export signals that control subcellular localization and transcriptional activity of ANCO-1 provide new insights toward a better understanding of the regulation of ANCO-1 activity.

ACKNOWLEDGMENTS

We thank Percy L. Yeung, Kai-H. Chang, and Gia K. Dinh for helpful discussion during the course of this study, and Michael Chisamore for critical reading of the manuscript. This work was supported by NIH grants DK52888, DK52542 and CA87074 (to J.D.C.). J.D.C. is a Research Scholar of the Leukemia and Lymphoma Society.

REFERENCES

Anzick SL, Kononen J, Walker RL, Azorsa DO, Tanner MM, Guan XY, Sauter G, Kallioniemi OP, Trent JM, Meltzer PS. 1997. AIB1, a steroid receptor coactivator amplified in breast and ovarian cancer. Science 277:965–968.

Behrends U, Schneider I, Rossler S, Frauenknecht H, Golbeck A, Lechner B, Eigenstetter G, Zobywalski C, Muller-Weihrich S, Graubner U, Schmid I, Sackerer D, Spath M, Goetz C, Prantl F, Asmuss HP, Bise K, Mautner J. 2003. Novel tumor antigens identified by autologous antibody screening of childhood medulloblastoma cDNA libraries. Int J Cancer 106:244–251.

Chen JD, Evans RM. 1995. A transcriptional co-repressor that interacts with nuclear hormone receptors [see comments]. Nature 377:454–457.

Chen H, Lin RJ, Schiltz RL, Chakravarti D, Nash A, Nagy L, Privalsky ML, Nakatani Y, Evans RM. 1997. Nuclear receptor coactivator ACTR is a novel histone acetyltransferase and forms a multimeric activation complex with P/CAF and CBP/p300. Cell 90:569–580.

Dyck JA, Maul GG, Miller WH, Jr., Chen JD, Kakizuka A, Evans RM. 1994. A novel macromolecular structure is a target of the promyelocyte-retinoic acid receptor oncoprotein. Cell 76:333–343.

Fukuda M, Asano S, Nakamura T, Adachi M, Yoshida M, Yanagida M, Nishida E. 1997. CRM1 is responsible for intracellular transport mediated by the nuclear export signal. Nature 390:308–311.

Ghosh JC, Yang X, Zhang A, Lambert MH, Li H, Xu HE, Chen JD. 2002. Interactions that determine the assembly of a retinoid X receptor/corepressor complex. Proc Natl Acad Sci USA 99:5842–5847.

Goldfarb DS, Corbett AH, Mason DA, Harreman MT, Adam SA. 2004. Importin alpha: A multipurpose nuclear-transport receptor. Trends Cell Biol 14:505–514.

Guenther MG, Lane WS, Fischle W, Verdin E, Lazar MA, Shiekhattar R. 2000. A core SMRT corepressor complex containing HDAC3 and TBL1, a WD40-repeat protein linked to deafness. Genes Dev 14:1048–1057.

Heery DM, Kalkhoven E, Hoare S, Parker MG. 1997. A signature motif in transcriptional co-activators mediates binding to nuclear receptors. Nature 387:733–736.

Henkel T, Zabel U, van Zee K, Muller JM, Fanning E, Baeuerle PA. 1992. Intramolecular masking of the nuclear location signal and dimerization domain in the precursor for the p50 NF-kappa B subunit. Cell 68:1121–1133.

Hong H, Kohli K, Trivedi A, Johnson DL, Stallcup MR. 1996. GRIP1, a novel mouse protein that serves as a transcriptional coactivator in yeast for the hormone binding domains of steroid receptors. Proc Natl Acad Sci USA 93:4948–4952.

Hong H, Kohli K, Garabedian MJ, Stallcup MR. 1997. GRIP1, a transcriptional coactivator for the AF-2 transactivation domain of steroid, thyroid, retinoid, and vitamin D receptors. Mol Cell Biol 17:2735–2744.

Horlein AJ, Naar AM, Heinzel T, Torchia J, Gloss B, Kurokawa R, Ryan A, Kamei Y, Soderstrom M, Glass CK, et al. 1995. Ligand-independent repression by the thyroid

hormone receptor mediated by a nuclear receptor co-repressor. Nature 377:397–404.

Huang W, Sun G-L, Li X-S, Cao Q, Lu Y, Jang G-S, Zahang F-Q, Chai J-R, Wang Z-Y, Waxman S, Chen Z, Chen S-J. 1993. Acute promyelocytic leukemia: Clinical relevance of two major PML-RARa isoforms and detection of minimal residual disease by retrotranscriptase/polymerase chain reaction to predict relapse. Blood 82:1264–1269.

Kudo N, Matsumori N, Taoka H, Fujiwara D, Schreiner EP, Wolff B, Yoshida M, Horinouchi S. 1999. Leptomycin B inactivates CRM1/exportin 1 by covalent modification at a cysteine residue in the central conserved region. Proc Natl Acad Sci USA 96:9112–9117.

Kutay U, Guttinger S. 2005. Leucine-rich nuclear-export signals: Born to be weak. Trends Cell Biol 15:121–124.

Leo C, Chen JD. 2000. The SRC family of nuclear receptor coactivators. Gene 245:1–11.

Li H, Gomes PJ, Chen JD. 1997. RAC3, a steroid/nuclear receptor-associated coactivator that is related to SRC-1 and TIF2. Proc Natl Acad Sci USA 94:8479–8484.

Li J, Wang J, Nawaz Z, Liu JM, Qin J, Wong J. 2000. Both corepressor proteins SMRT and N-CoR exist in large protein complexes containing HDAC3 [In Process Citation]. EMBO J 19:4342–4350.

Mangelsdorf DJ, Thummel C, Beato M, Herrlich P, Schtz G, Umesono K, Blumberg B, Kastner P, Mark M, Chambon P, Evans RM. 1995. The nuclear receptor superfamily: The second decade. Cell 83:835–839.

Nagy L, Kao HY, Chakravarti D, Lin RJ, Hassig CA, Ayer DE, Schreiber SL, Evans RM. 1997. Nuclear receptor repression mediated by a complex containing SMRT, mSin3A, and histone deacetylase. Cell 89:373–380.

Nawaz Z, Baniahmad C, Burris TP, Stillman DJ, O'Malley BW, Tsai MJ. 1994. The yeast SIN3 gene product negatively regulates the activity of the human progesterone receptor and positively regulates the activities of GAL4 and the HAP1 activator. Mol Gen Genet 245:724–733.

Ordentlich P, Downes M, Xie W, Genin A, Spinner NB, Evans RM. 1999. Unique forms of human and mouse nuclear receptor corepressor SMRT. Proc Natl Acad Sci USA 96:2639–2644.

Oñate SA, Tsai SY, Tsai MJ, O'Malley BW. 1995. Sequence and characterization of a coactivator for the steroid hormone receptor superfamily. Science 270:1354–1357.

Park EJ, Schroen DJ, Yang M, Li H, Li L, Chen JD. 1999. SMRTe, a silencing mediator for retinoid and thyroid hormone receptors-extended isoform that is more related to the nuclear receptor corepressor. Proc Natl Acad Sci USA 96:3519–3524.

Powell JA, Gardner AE, Bais AJ, Hinze SJ, Baker E, Whitmore S, Crawford J, Kochetkova M, Spendlove HE, Doggett NA, Sutherland GR, Callen DF, Kremmidiotis G. 2002. Sequencing, transcript identification, and quantitative gene expression profiling in the breast cancer loss of heterozygosity region 16q24.3 reveal three potential tumor-suppressor genes. Genomics 80:303–310.

Sessler RJ, Noy N. 2005. A ligand-activated nuclear localization signal in cellular retinoic acid binding protein-II. Mol Cell 18:343–353.

Shiau AK, Barstad D, Loria PM, Cheng L, Kushner PJ, Agard DA, Greene GL. 1998. The structural basis of estrogen receptor/coactivator recognition and the antagonism of this interaction by tamoxifen. Cell 95:927–937.

Smith JM, Koopman PA. 2004. The ins and outs of transcriptional control: Nucleocytoplasmic shuttling in development and disease. Trends Genet 20:4–8.

Takeshita A, Cardona GR, Koibuchi N, Suen CS, Chin WW. 1997. TRAM-1, A novel 160-kDa thyroid hormone receptor activator molecule, exhibits distinct properties from steroid receptor coactivator-1. J Biol Chem 272: 27629–2734.

Tikkanen MK, Carter DJ, Harris AM, Le HM, Azorsa DO, Meltzer PS, Murdoch FE. 2000. Endogenously expressed estrogen receptor and coactivator AIB1 interact in MCF-7 human breast cancer cells. Proc Natl Acad Sci USA 97:12536–12540.

Torchia J, Rose DW, Inostroza J, Kamei Y, Westin S, Glass CK, Rosenfeld MG. 1997. The transcriptional co-activator p/CIP binds CBP and mediates nuclear-receptor function [see comments]. Nature 387:677–684.

Voegel JJ, Heine MJS, Zechel C, Chambon P, Gronemeyer H. 1996. TIF2, a 160 kDa transcriptional mediator for the ligand-dependent activation function AF-2 of nuclear receptors. EMBO J 15:3667–3675.

Wang Z, Rose DW, Hermanson O, Liu F, Herman T, Wu W, Szeto D, Gleiberman A, Krones A, Pratt K, Rosenfeld R, Glass CK, Rosenfeld MG. 2000. Regulation of somatic growth by the p160 coactivator p/CIP. Proc Natl Acad Sci USA 97:13549–13554.

Weis K. 2003. Regulating access to the genome: Nucleocytoplasmic transport throughout the cell cycle. Cell 112: 441–451.

Weis K, Rambaud S, Lavau C, Jansen J, Carvalho T, Carmo-Fonseca M, Lamond A, Dejean A. 1994. Retinoic acid regulates aberrant nuclear localization of PML-RAR alpha in acute promyelocytic leukemia cells. Cell 76:345–356.

Xu J, Qiu Y, DeMayo FJ, Tsai SY, Tsai MJ, O'Malley BW. 1998. Partial hormone resistance in mice with disruption of the steroid receptor coactivator-1 (SRC-1) gene. Science 279:1922–1925.

Xu J, Liao L, Ning G, Yoshida-Komiya H, Deng C, O'Malley BW. 2000. The steroid receptor coactivator SRC-3 (p/CIP/RAC3/AIB1/ACTR/TRAM-1) is required for normal growth, puberty, female reproductive function, and mammary gland development. Proc Natl Acad Sci USA 97:6379–6384.

Xu HE, Stanley TB, Montana VG, Lambert MH, Shearer BG, Cobb JE, McKee DD, Galardi CM, Plunket KD, Nolte RT, Parks DJ, Moore JT, Kliewer SA, Willson TM, Stimmel JB. 2002. Structural basis for antagonist-mediated recruitment of nuclear co-repressors by PPAR-alpha. Nature 415:813–817.

Zhang A, Yeung PL, Li CW, Tsai SC, Dinh GK, Wu X, Li H, Chen JD. 2004. Identification of a novel family of ankyrin repeats containing cofactors for p160 nuclear receptor coactivators. J Biol Chem 279:33799–33805.